Biology of Reproduction, 2023, **109(1)**, 53–64
https://doi.org/10.1093/biolre/ioad050
Advance access publication date 8 May 2023
Research Article

Aerobic exercises regulate the epididymal anion homeostasis of high-fat diet-induced obese rats through TRPA1-mediated Cl^- and HCO_3^- secretion†

Dong-Dong Gao[1,*,‡], Nan Ding[1,‡], Wei-Ji Deng[1], Pei-Lun Li[1], Yi-Lin Chen[1], Lian-Meng Guo[1], Wen-Hao Liang[1], Jia-Hui Zhong[1], Jing-Wen Liao[1], Jun-Hao Huang[1,2,*] and Min Hu[1,*]

[1]Guangdong Provincial Key Laboratory of Physical Activity and Health Promotion, Scientific Research Center, Guangzhou Sport University, Guangzhou, Guangdong, China
[2]Dr Neher's Biophysics Laboratory for Innovative Drug Discovery, State Key Laboratory of Quality Research in Chinese Medicine, Macau University of Science and Technology, Macau, China

*__Correspondence:__ Huang Guangdong Provincial Key Laboratory of Physical Activity and Health Promotion, Scientific Research Center, Guangzhou Sport University, 1268 Middle Guangzhou Avenue, Guangzhou 510500, China. E-mail: gaodd@gzsport.edu.cn; junhaohuang2006@hotmail.com; minhu@gzsport.edu.cn

†__Grant Support:__ This study is supported by the Guangdong Basic and Applied Basic Research Foundation (No. 2021A1515011264, 2023A1515012011), the Guangzhou Science and Technology Planning Project (2023A04J0150), the National Natural Science Foundation of China (grant number 31600969), and the Macao Science and Technology Development Fund (Project code: 001/2020/ALC).

‡Dong-Dong Gao and Nan Ding contributed equally to this work.

Abstract

Aerobic exercises could improve the sperm motility of obese individuals. However, the underlying mechanism has not been fully elucidated, especially the possible involvement of the epididymis in which sperm acquire their fertilizing capacity. This study aims to investigate the benefit effect of aerobic exercises on the epididymal luminal milieu of obese rats. *Sprague–Dawley* male rats were fed on a normal or high-fat diet (HFD) for 10 weeks and then subjected to aerobic exercises for 12 weeks. We verified that TRPA1 was located in the epididymal epithelium. Notably, aerobic exercises reversed the downregulated TRPA1 in the epididymis of HFD-induced obese rats, thus improving sperm fertilizing capacity and Cl^- concentration in epididymal milieu. Ussing chamber experiments showed that cinnamaldehyd (CIN), agonist of TRPA1, stimulated an increase of the short-circuit current (I_{SC}) in rat cauda epididymal epithelium, which was subsequently abolished by removing the ambient Cl^- and HCO_3^-. *In vivo* data revealed that aerobic exercises increased the CIN-stimulated Cl^- secretion rate of epididymal epithelium in obese rats. Pharmacological experiments revealed that blocking cystic fibrosis transmembrane regulator (CFTR) and Ca^{2+}-activated Cl^- channel (CaCC) suppressed the CIN-stimulated anion secretion. Moreover, CIN application in rat cauda epididymal epithelial cells elevated intracellular Ca^{2+} level, and thus activate CACC. Interfering with the PGHS2-PGE2-EP2/EP4-cAMP pathway suppressed CFTR-mediated anion secretion. This study demonstrates that TRPA1 activation can stimulate anion secretion via CFTR and CaCC, which potentially forming an appropriate microenvironment essential for sperm maturation, and aerobic exercises can reverse the downregulation of TRPA1 in the epididymal epithelium of obese rats.

Received: February 8, 2023. **Revised:** April 19, 2023. **Accepted:** May 2, 2023.

Graphical Abstract

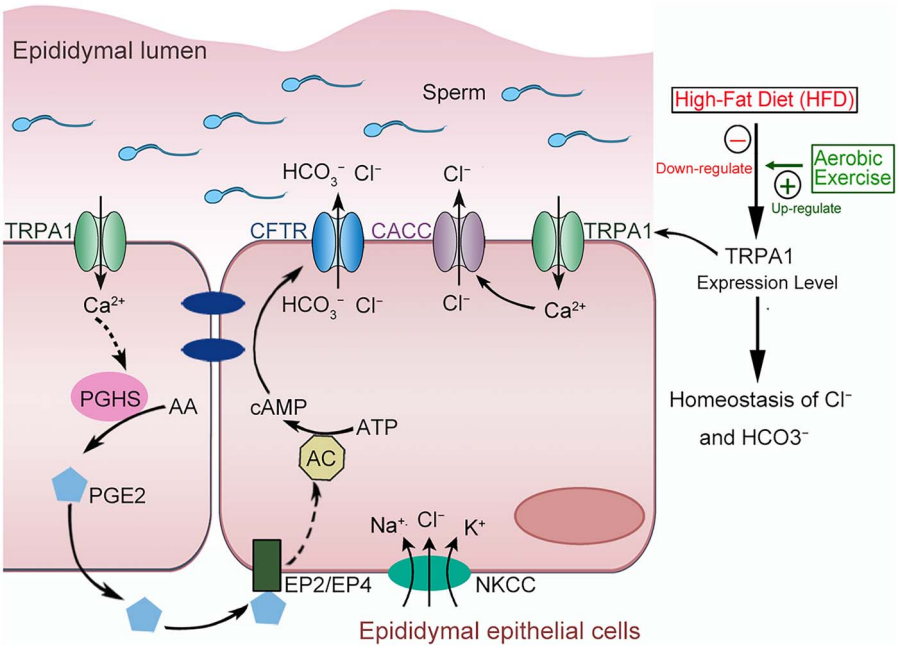

Keywords: aerobic exercises, high-fat diet, TRPA1, epididymal epithelium, anion secretion

Introduction

Dysfunction of the male reproductive system is a common complication of obesity [1]. Nearly 80% of male patients with reproductive disorders are classified as overweight or obesity [2]. Obesity leads to erectile dysfunction and poor semen quality, including decreased sperm concentration, abnormal sperm morphology, impaired sperm motility and fertilizing capacity, and subclinical prostatitis [3, 4]. Its pathogenic reasons can be attributed to the disorders of the hypothalamic–pituitary–gonadal axis, oxidative stress, glucose and lipid metabolism disorders, leptin resistance, dysbiosis of gut microbes, inflammation, and many other aspects [5–8].

Unlike many other diseases, obesity and its complications can be counteracted by lifestyle changes. Moderate physical activity can reverse the pathological phenotypes of obese individuals [9]. Several studies postulate that physical exercises can reverse imbalanced sperm parameters, including the decline of sperm concentration and sperm motility in obese individuals [8, 10, 11]. These findings suggest that obesity affects spermatogenesis in the testis and the subsequent sperm maturation in the epididymis. The effects of obesity and lack of physical exercises on spermatogenesis in the testis have been well documented over the past decades [12–14]. Martini et al. analyzed the levels of A-glucosidase (NAG) in seminal plasma and proposed that the decrease of sperm motility in obese individuals is caused by the disorder of epididymal function [15]. A few studies reported that obesity leaded to the increased local inflammation, oxidative stress level of epididymis, and the reduction in sperm storage time in the epididymis [8, 16]. However, the effect of obesity on the sperm maturation in epididymis and its underlying mechanism remain largely unknown. The optimal lumen microenvironment, characterized by the specific concentration of Ca^{2+}, Na^+, Cl^-, HCO_3^-, and K^+, which is established by the active vectorial ion transport by the epididymal epithelium, is the basis for sperms to acquire motility and fertilization ability during transit in the epididymis [17]. Previous studies postulated that a dysfunction of the transepithelial absorption or secretion of Ca^{2+}, Cl^-, HCO_3^-, and K^+ resulted in the decline of epididymal sperm motility [18, 19]. However, it is not yet clear whether physical exercises can improve sperm motility and fertilizing capacity by reversing the epididymal epithelial ion transport disorder in HFD-induced obese rats.

The transient receptor potential ankyrin 1 (TRPA1), a calcium-permeable non-selective cation channel, has been demonstrated to be associated with the pathological process of obesity and female infertility [20, 21]. TRPA1 is also associated with spermatogenesis in the male reproductive system of vertebrates [22]. Obesity causes the up or downregulation of TRPA1expression level in various tissues [23–25], suggesting TRPA1 may represent an effective potential therapeutic target of obesity. Besides, TRPA1 activation stimulates remarkable transepithelial Cl^- and HCO_3^- secretion in colon [26, 27]. These reports suggest a potential role of TRPA1 in the anion secretion of epididymal epithelium and the dysfunction of the transepithelial anion secretion induced by the HFD. However, the TRPA1 expression pattern and its function in the epididymis remain unknown.

This study thus aims to investigate the effect of HFD and subsequent physical exercises on the TRPA1 expression level in the epididymal epithelium, to reveal the underlying cellular mechanisms of the pre-secretion function of TRPA1. This study will uncover TRPA1 as a potential target of physical exercises-based improvement of epididymal sperm motility and fertilizing capacity in HFD-induced obese rats.

Materials and methods

Animals

Male *Sprague–Dawley* (SD) rats (weight 100–120 g) were purchased from the Guangdong Medical Laboratory Animal Center (Guangzhou, China). Rats were fed with 60 kcal% from fat diet (5.24 kcal/g) for 10 weeks as the high-fat diet (HFD) group and fed with 10 kcal% from fat diet (3.85 kcal/g) as the control group. Rats with body weight 20% higher than that of the control group, and the Lee's index was 1.5% higher than that of the control group were judged as obese rats. Subsequently, rats were randomly assigned to the Normal diet control group (NC group), the Normal diet with exercises group (NE group), the HFD control *group* (HC group), and the HFD with *exercises group* (HE group). Exercises training of the rats was performed for 1 h/day and 5 days/week for 12 weeks on a treadmill. The exercises training protocol consist of 15 m/min (moderate-intensity, 55–65% VO_2max, 40 min) with 0% grade, and 20 min warm-up and cool-down periods. All animal experimental procedures received ethical approval and were performed according to the guidelines of the Animal Experimentation Ethics Committee of Guangzhou Sport University.

Chemicals and solutions

Minimum essential medium (MEM), F10 medium, fetal bovine serum, penicillin/streptomycin, Hanks Balanced Salt Solution, and 0.25% trypsin were purchased from Gibco (Carlsbad, CA, USA). Chlortetracycline (CTC) was purchased from Amresco (Solon, OH, USA). 5-alpha-dihydrotestosterone (5a-DHT), collagenase IA, bumetanide (Bum), 4-(2-hydroxyethyl)-1-piperazineethanesulfonic acid (HEPES), bovine serum albumin (BSA), CFTRinh-172, 4′-diisothiocyanostilbene-2, 2′- disulphonic acid (DIDS), AH-6809, AH-23848, forskolin (FSK), MDL-12330A, indomethacin, piroxicam, Ethylene glycol-bis(2-aminoethylether)-N,N,N′,N′-tetraacetic acid A (EGTA), and dimethyl sulfoxide (DMSO) were purchased from Sigma-Aldrich (St. Louis, MO, USA). Cinnamaldehyd (CIN), HC-030031 Thapsigargin (Tg) were purchased from MedChemExpress (New Jersey, USA). Fluo-4 a.m. was purchased from Molecular Probes (Eugene, OR, USA). NaCl, KCl, $MgSO_4$, HCl, $BaCl_2$, $NaHCO_3$, KH_2PO_4, $CaCl_2$, and glucose were purchased from Guangzhou Chemical Pharmaceutical Factory (Guangzhou, China). Normal Krebs–Henseleit (K–H) solution contained 117 mM NaCl, 4.7 mM KCl, 2.5 mM $CaCl_2$, 1.2 mM $MgCl_2$, 24.8 mM $NaHCO_3$, 1.2 mM KH_2PO_4, and 11.1 mM glucose. In Cl^- free K–H solution, ambient NaCl, KCl, and $CaCl_2$ were replaced by Na-gluconate, K-gluconate, Ca-gluconate. The solution was gassed with 95% O_2 and 5% CO_2 at 32°C to attain a pH of 7.4. In HCO_3^- free K–H solution, $NaHCO_3$ was replaced by 10 mM HEPES to sustain a pH of 7.4, and additional 24.8 mM NaCl was supplemented. In Cl^- and HCO_3^- both-free K–H solution, Cl^- was replaced by gluconate and $NaHCO_3$ was replaced by HEPES. The solution was bubbled with 100% O_2 to avoid carrying HCO_3^- into the solution. Normal physiological saline solution (N-PSS) contained 137 mM NaCl, 5 mM KCl, 1 mM $MgCl_2$, 2.5 mM $CaCl_2$, 10 mM HEPES, and 10 mM glucose. The Ca^{2+}-free PSS was prepared by omitting Ca^{2+} and adding 2 mM EGTA.

Computer aided sperm motion analysis

The cauda epididymal sperm were collected as described before [18]. After collection, the sperm were incubated in F10 solution at 37°C for 10 min. The motility parameters including the percentage of motile and forward progressives from the total sperm analyzed were measured by computer aided sperm motion analysis system (SCA V 5.2, MICROPTIC S.L. Viladomat, Barcelona, Spain). The "*n*" value represents the number of independent experiments.

CTC fluorescence assay

The capacitation and acrosome reaction of rat sperm was detected by CTC staining as described previously [28], with a few modifications. Briefly, CTC was dissolved in a buffer containing 20 mM Tris–HCl, 5 mM cysteine, and 130 mM NaCl (pH 7.8) at a concentration of 500 μM. Sperm were incubated in capacitation medium Biggers, Whitter and Whittingham (BWW) solution for 1 h. Then the sperm suspension and CTC solution were mixed with equal volume. After 20 s, the sperm were fixed by adding 8 μl 12.5% glutaraldehyde in 2 M Tris–HCl buffer (pH 7.8). Subsequently, the sperm suspension was washed by PBS and centrifugated at 200 × g for 5 min. The pellet was then resuspended in 100 μl PBS, and the suspension was placed on a clear slide. The F pattern represented incapacitated sperm, the B pattern represented capacitated and acrosome-intact sperm, and the AR pattern represented capacitated and acrosome reacted sperm. The "*n*" value represents the number of independent experiments, and >200 sperms were counted to assess the different CTC staining patterns in each independent experiment.

Real-time quantitative PCR

Total ribonucleic acid (RNA) of rat cauda epididymal tissues was extracted using RNAprep pure Tissue Kit (TIANGEN BIOTECH, Beijing, China). Real-time quantitative PCR (qPCR) was performed using the SYBR Green I testing system (TOYOBO, Osaka, Japan) according to the manufacturer's protocol. The qPCR conditions consisted of 40 cycles of denaturation at 95°C for 5 s, annealing at 58°C for 10 s, and polymerization at 60°C for 30 s. Specific primer sequences were as follow: *Trpa1* forward primer, 5′- ATCCGAATAGACCCAGGCAC-3′, *Trpa1* reverse primer, 5′- TGAGGTCCTTCAGCCGGTAT-3′; *β-actin* forward primer, 5′-AGCTGAGAGGGAAATCGTGC-3′, *β-actin* reverse primer, 5′-GGAACCGCTCATTGCCGATA-3′. The "*n*" value represents the number of independent experiments.

Western blot analysis

Total protein extract was obtained from rat cauda epididymal tissues. The epididymal protein was resolved by sodium dodecyl-sulfate-polyacrylamide gel electrophoresis (SDS-PAGE) and then transferred onto a poly(vinylidene fluoride)(PVDF) membrane. After blocking with 5% (w/v) BSA for 1 h at room temperature, the PVDF membranes were incubated with an anti-TRPA1 antibody (1:1000; PA5-88615; Thermo Fisher Scientific) overnight at 4°C. The PVDF membranes were then incubated with a horseradish peroxidase (HRP)-conjugated secondary antibody (1:20 000, EarthOx, Millbrae) for 1 h at room temperature. A HRP substrate kit (Tanon, Shanghai, China) was employed to visualize the target proteins.

Immunofluorescence analysis

A standard immunohistochemical method was used to label the paraffin sections of rat caput, corpus, and cauda epididymal tissues as described previously [18]. The sections

were incubated with an anti-TRPA1 antibody (1:1500; PA5-88615; Thermo Fisher Scientific) at 4°C overnight; negative controls were obtained by incubating the sections with PBS only. After incubation with the fluorescein isothiocyanate-conjugated secondary antibody, the images were captured by a scanning system (KF-400, KFBIO).

Primary culture of rat cauda epididymal epithelial cells

The primary culture of rat cauda epididymal epithelial cells was performed as described previously [29]. In brief, eight male SDrats (weight 100–120 g) were sacrificed by CO_2 asphyxiation. The cauda epididymis was finely minced with scissors and subjected to enzymic digestion with 0.25% (w/v) trypsin and 0.1% (w/v) collagenase IA. The disaggregated cell mass was then suspended in a medium containing MEM (88% v/v), sodium pyruvate (1 mM), 5a-DHT (1 nM), FBS (10% v/v), penicillin (100 IU/mL), and streptomycin (100 IU/mL). The cells were cultured for 4–6 h, then the non-adherent epithelial cell suspension was seeded onto Millipore filters (0.45 μM) or coverslips for further investigation. The cells were incubated at 32°C with 5% CO_2 for 3–4 days until the monolayers reached confluence and were then used for the measurement of the short-circuit current (I_{SC}).

Measurement of the I_{SC}

The Ussing chamber experiments were performed as described previously [30]. In Brief, the monolayers were vertically clamped in the Ussing chamber, with a perfusion system to maintain the system at 32°C. The voltage-clamp amplifier (VCC MC6, Physiologic Instruments, San Diego, CA, USA) employed to short-circuit the monolayer, and a signal collection and analysis system (BL-420E+, Chengdu Technology & Market, Chengdu, China) used to obtain real-time I_{SC} data. Transepithelial resistance was calculated from Ohm's law and the change of I_{SC} was defined as the altered I_{SC} value which was normalized to current change per unit area of themonolayer ($\Delta\mu A/cm^2$). In pharmacological experiments, inhibitors, or blockers were added 20 min before the administration of CIN. The I_{SC} response was expressed as upward when the anions flowed from the basal to the apical side of the epithelium, or the cations flowed from the apical to the basal side of the epithelium. The "*n*" value represents the number of independent experiments.

In vivo measurement of Cl^- secretion rate of rat cauda epididymal epithelium

Microperfusion of rat cauda epididymis was performed as previously described [18], with a few modifications. SD rats were anesthetized through intraperitoneal injection of 3% pentobarbital sodium (0.15 ml/100 g of body weight) to maintain the animals under anesthesia. Cauda epididymis from both sides of the animal was cannulated with tailor-made catheters (diameter 100–200 μm). The original cauda epididymal lumen fluid was collected and then centrifuge (6000 g) for 10 min at 4°C, the supernatant was collected to measure the concentration of Cl^-. The cauda epididymal lumen was then perfused the solution (N-PSS) use an infusion pump (LongerPump, Baoding, China) at a rate of 10 ml/min. After perfusion for 30 min, the perfusate was then collected into a 1.5-ml tube through the vas deferens inserted with a polyethylene tubing (for 60 min). The samples were then diluted and filtered through a 0.22 mm pore filter. The concentration of Cl^- was analyzed by ion chromatography (ICS-900, Dionex, Sunnyvale, CA, USA). The length of the epididymal lumen that receives perfusion was measured to calibrate the Cl^- secretion rate. The "*n*" value represents the number of independent experiments.

Measurement of the intracellular Ca^{2+} concentration ($[Ca^{2+}]_i$)

The primary cultured cells on cover-slips were washed with N-PSS or Ca^{2+}-free PSS three times and then incubated with fluo-4 a.m. (10 μM) for 40 min at 32°C. Cover-slips were then transferred to a 1 ml chamber perfused with N-PSS or Ca^{2+}-free PSS and the fluorescence signal was recorded using a laser scanning confocal imaging system (TCS SP2, Leica Microsystems, Mannheim, Germany). The fluorescence intensity after drug treatment was normalized to the initial intensity (% of initial intensity). The "*n*" value represents the number of independent experiments, and >20 cells were evaluated in each independent experiment.

Measurement of the intracellular cAMP concentration ($[cAMP]_i$)

Primary cultured rat cauda epididymal epithelial cells were grown in 12-well culture plates for 3 days. The content of the $[cAMP]_i$ in the rat cauda epididymal epithelial cells lysates was detected using the cAMP enzyme immunoassay kit (KGE004B, R&D Systems, USA) according to the manufacturer's instructions. BCA Protein Assay Kit (C503021, Sangon Biotech, China) was used to measure the protein content of the cell lysates. The "*n*" value represents the number of independent samples.

Detection of PGE2 generation

Cells grown in 12-well culture plates were refreshed by the serum-free medium, and inhibitors, or blockers were added 20 min before the administration of CIN. After incubating with CIN for another 8–10 min, 900 μl of supernatant were collected and centrifuged (4°C, 6000 g) to remove cellular debris. PGE2 content in the supernatant was measured using the PGE2 enzyme-linked immunosorbent assay (ELISA) kit following the manufacturer's instructions. BCA Protein Assay Kit (C503021, Sangon Biotech, China) was used to measure the protein content of the cell lysates. The "*n*" value represents the number of independent samples.

Data analysis and statistics

Our data were statistically analyzed by GraphPad Prism 8.0 (GraphPad Software, CA, USA). The results were presented as means ± S.D. One-way analysis-of-variance (ANOVA) with Bonferroni analysis was performed to assess the differences between three or more groups. A value of $P < 0.05$ was considered to be statistically significant.

Results

Aerobic exercises reverse the decline of sperm fertilizing capacity and the epididymal TRPA1 expression level of HFD-induced obese rats

The sperm motile parameters, including the percentage of motile sperm and the forward progressives, and the ability of capacitation were both significantly decreased in the HFD-induced obese male rats (Figure 1A–D). However, aerobic exercises reversed this decline, suggesting that the epididymis

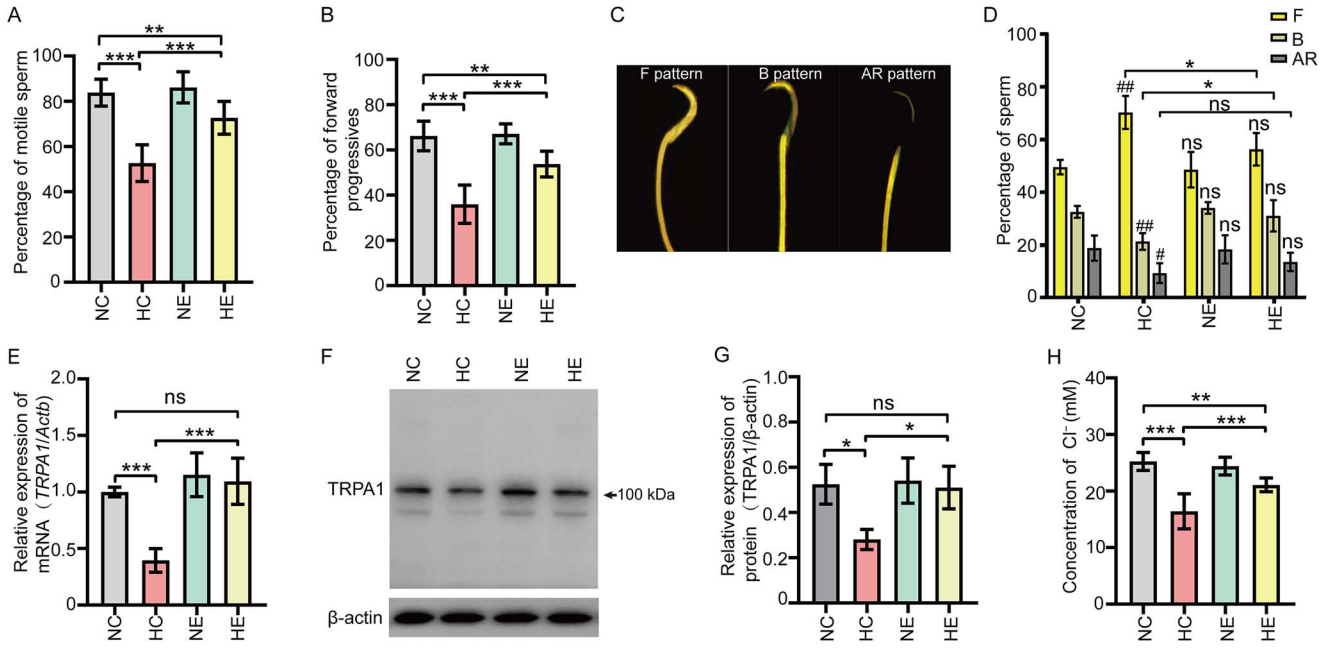

Figure 1. Aerobic exercises reverse the decline of sperm fertilizing capacity and the epididymal TRPA1 expression level of obese rat. (A) and (B) Statistical analysis showing the sperm motility parameters of rat models ($n = 12$). (C) CTC fluorescence image showing the acrosome-reacted (AR pattern), capacitated (B pattern), or non-capacitated (F pattern) rat sperm. (D) The statistical analysis showing the percentage of F, B, and AR pattern sperm ($n = 4$). $^{\#}P < 0.05$, $^{\#\#}P < 0.01$versus the NC group, ns represents no significance. (E) Statistical analysis showing the relative mRNA level of *TRPA1* in cauda epididymis of rat models ($n = 4$), β-actin (*Actb*) was used as an internal control. (F) Western blot analysis showing the expression level of TRPA1 protein in cauda epididymis obtained from rat models. (G) Statistical analysis showing the relative protein level of TRPA1 in cauda epididymis of rat models ($n = 3$). (H) Statistical analysis showing the Cl^- concentration in the cauda epididymal lumen of rat models ($n = 8$). $^{*}P < 0.05$, $^{**}P < 0.01$, $^{***}P < 0.001$, ns represents no significance. Symbols and bars indicated the means ± SD.

is potentially the target organ of aerobic exercises. Notably, the mRNA and protein levels of TRPA1 were decreased in the cauda epididymis of HFD-induced obese rats, and the decline tendency were reversed by 12-week aerobic exercises (Figure 1E–G). Furthermore, our data showed that aerobic exercises improved the decline of the Cl^- concentration in the epididymis luminal fluid in obese male rats (Figure 1H).

Activation of TRPA1 stimulates anion secretion of rat epididymal epithelium

The possible involvement of TRPA1 in the regulation of Cl^- homeostasis was then investigated. The localization of TRPA1 in rat epididymis was detected using IF analysis. The positive labeling of TRPA1 was detected in the epithelial layer of the rat epididymal duct (Figure 2A–D). Ussing chamber experiments were then employed to explore the pro-secretion role of TRPA1 in rat epididymal epithelial cells. The transepithelial electrical resistance value of primary cultured cauda epididymal epithelialmonolayer was $892.89 \pm 169.70\ \Omega \times cm^2$ ($n = 18$), with a basal I_{SC} value of $2.38 \pm 0.61\ \mu A/cm^2$ ($n = 18$) in normal K–H solution under the unstimulated state. Application of TRPA1 activator CIN (1 mM, AP) in epididymal epithelial cells triggered a substantial increase in I_{SC}, while the vehicle DMSO (0.2% v/v, AP) failed to affect the I_{SC} (Figure 2E, F, & H), and the CIN-stimulated I_{SC} response was abolished when the monolayer was pretreated with TRPA1 selective blocker HC030031(100 μM, AP) (Figure 2G & H).

A series of ion substitution experiments were then employed to determine the ion composition involved in the CIN-stimulated *I*sc response. The *I*sc responses evoked by CIN were significantly inhibited in Cl^- free K–H solution, HCO_3^- free K–H solution, and Cl^- & HCO_3^- free K–H solution (Figure 3A–E). These data demonstrated that CIN-stimulated *I*sc response was transepithelial secretion of Cl^- and HCO_3^-. The secretion rate of Cl^- induced by the activation of TRPA1 was further detected *in vivo* using microperfusion of rat cauda epididymal tubule. The calculated rate of the Cl^- secretion was 7.56 ± 1.19 nmol/cm^2/min ($n = 8$) in the NC group and 16.01 ± 2.27 nmol/cm^2/min ($n = 8$) when CIN (1 mM) was applied (Figure 3F). Moreover, CIN-stimulated Cl^- secretion rate was significantly decreased in HC groups (9.94 ± 2.20 nmol/cm^2/min, $n = 8$) compared to that in HE groups (15.59 ± 3.11 nmol/cm^2/min, $n = 8$). These data suggested that aerobic exercises reversed the downregulated TRPA1 expression level in the epididymal epithelium of HFD-induced obese rats, thus promoting anion secretion.

CACC and CFTR are involved in CIN-stimulated anion secretion

Cystic fibrosis transmembrane regulator (CFTR) and Ca^{2+}-activated Cl^- channel (CACC) expressed in the epididymal epithelial cells and functioned as anion channels, which were responsible for anion secretion. Thus, we sought to investigate the putative involvement of CFTR and CACC in CIN-stimulated anion secretion. The CIN-stimulated anion secretion was significantly attenuated when the monolayer was pretreated with CFTRinh-172 (10 μM, AP), a selective blocker of CFTR, or CaCC blocker DIDS (100 μM, AP) (Figure 4A, B, & E). Notably, the CIN-stimulated anion secretion was almost abolished when the monolayer was pretreated with CFTRinh-172 and DIDS (Figure 4C & E). In addition, basolateral Na^+-K^+-$2Cl^-$ cotransporter (NKCC)

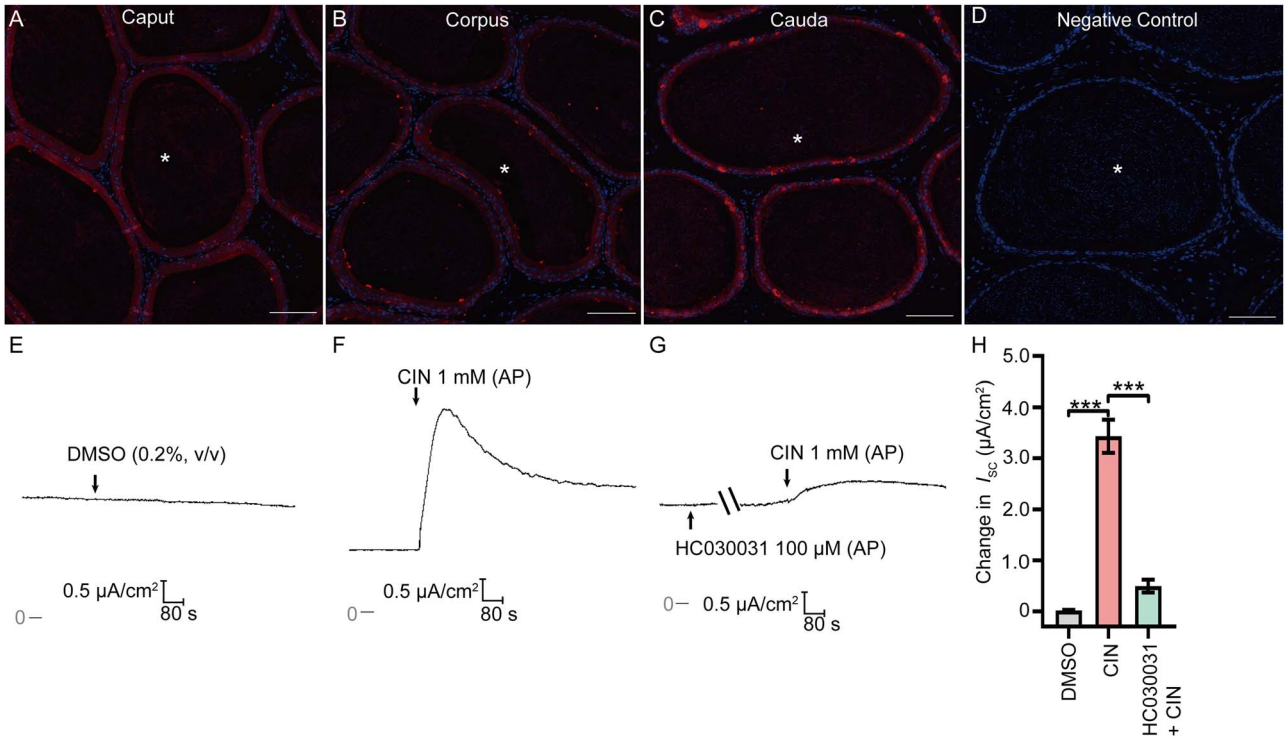

Figure 2. Activation of TRPA1 stimulate short-circuit current (Isc) responses in the rat epididymal epithelium. (A)–(C) The immunofluorescent labeling of TRPA1 in rat caupt, corpus and cauda epididymis sections. The red signal representing TRPA1(CY3-labeled) immunoreactivity. (D) Negative controls were prepared by substituting the primary antibody with PBS. Scale bars: 100 μm. (E) and (F) Representative traces showing the effects of DMSO (0.2% v/v, AP), CIN (1 mM, AP) on I_{SC} responses. (G) Representative trace showing the effect of HC030031 (100 μM, AP), the selective blocker of TRPA1, on CIN-induced I_{SC} response. (H) Statistical analysis showing the effects of DMSO, CIN or CIN (in the presence of HC030031) on the I_{SC} responses ($n = 4$–6). $^{***}P < 0.001$. Symbols and bars indicated the means ± SD.

was also indispensable for transepithelial ion transport. Pretreating the monolayer with bumetanide (100 μM, BL) significantly attenuated CIN-stimulated anion secretion (Figure 4D & E), highlighting the involvement of CFTR, CaCC, and basolateral NKCC in CIN-stimulated anion secretion.

Activation of TRPA1 stimulates Ca^{2+} influx in epididymal epithelial cells

We investigated the effect of CIN on $[Ca^{2+}]_i$ in rat cauda epididymal epithelial cells, given that TRPA1 is a nonselective cation channel that allows the influx of Ca^{2+}. We found that CIN (1 mM) induced an increase in $[Ca^{2+}]_i$ (Figure 5A & D), which was suppressed by pretreating the cells with TRPA1 selective blocker HC030031 (Figure 5B & D). Meanwhile, CIN (1 mM)-induced increase of $[Ca^{2+}]_i$ was abolished by the removal of ambient Ca^{2+} (Figure 5C & D). These findings indicated that activation of TRPA1 could elevate $[Ca^{2+}]_i$ via extracellular Ca^{2+} influx in rat cauda epididymal epithelial cells, subsequently activating CaCC and triggering Cl^- secretion.

The PGHS2-PGE2-EP2/EP4-AC-cAMP pathway is involved in the activation of CFTR

CFTR was activated by an increase in the intracellular cAMP level. The agonist of adenylate cyclase (AC), FSK, and the inhibitor of AC, MDL-12330A, were then applied to confirm the involvement of the AC-cAMP-CFTR pathway in CIN-stimulated anion secretion. As illustrated, CIN-stimulated Cl^- and HCO_3^- secretion was significantly decreased when the monolayer was pretreated with FSK (10 μM, AP) or MDL-12330A (10 μM, AP) (Figure 6A–C). Moreover, activation of TRPA1 significantly increased the [cAMP]i, which was eliminated by pretreating the cells with TRPA1 blocker HC030031, AC inhibitor MDL-12330A, and the PGE2 receptor-EP2/EP4 antagonists AH-6809 and AH-23848 (Figure 6D). These data demonstrated that the TRPA1-EP2/EP4-AC-cAMP pathway participates in the downstream signal transduction of TRPA1 activation.

The possible involvement of prostaglandin H synthase-2 (PGHS2)-PGE2-EP2/EP4 pathway after the TRPA1 activation was subsequently evaluated. The CIN-stimulated anion secretion was significantly decreased when the monolayer was pretreated with the nonselective PGHS2 inhibitor indomethacin (10 μM, AP) or piroxicam (10 μM, AP) (Figure 7A, B, & F). Pretreating the monolayer with the nonselective EP2 antagonist AH-6809 (20 μM, BL) or/and the nonselective EP4 antagonist AH-23848 (20 μM, BL) significantly suppressed the CIN-stimulated anion secretion (Figure 7C–F). Then, we further assessed the PGE2 content released by epididymal epithelial cells after the activation of TRPA1 to validate our hypothesis. Activation of TRPA1 significantly increased PGE2 release from the primary cultured rat cauda epididymal epithelial cells, but the increase was reversed by pretreating the cells with TRPA1 blocker HC030031 (100 μM), PGHS2 inhibitor indomethacin (10 μM), or piroxicam (10 μM) (Figure 7G).

Discussion

The pivotal role of lifestyle factors in male fertility, including diet and physical exercises, has generated considerable interest. It is universally accepted that physical exercises lead

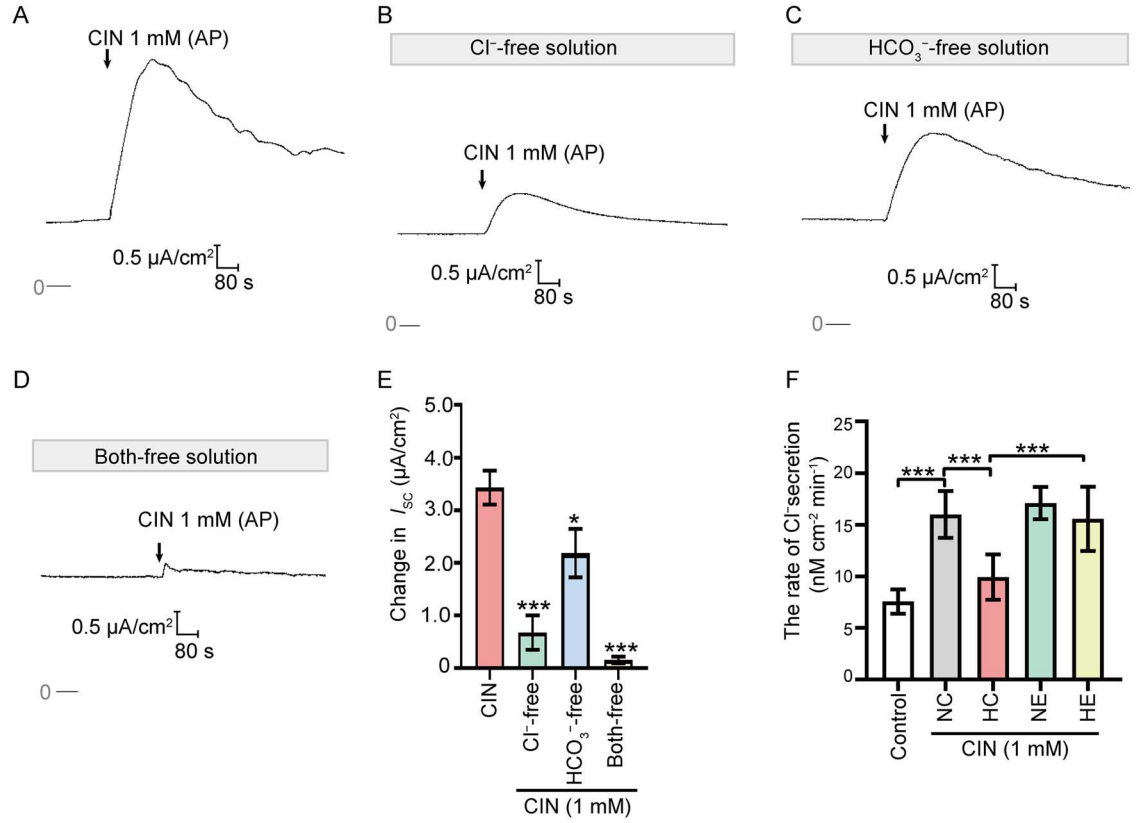

Figure 3. Activation of TRPA1 stimulated transepithelial Cl^- and HCO_3^- secretion. (A-D) Representative traces showing the effects of CIN (1 mM, AP) induced I_{SC} responses in normal K–H solution, Cl^- free K–H solution, HCO_3^- free K–H solution, Cl^- and HCO_3^- free K-H solution. (E) Statistical analysis showing the I_{SC} responses elicited by CIN in different bath solutions ($n = 4$–6), $^*P < 0.05$, $^{***}P < 0.001$ versus the CIN group. (F) Statistical analysis showing the Cl^- secretion rate of cauda epididymal tubule of different rat models ($n = 8$). $^*P < 0.05$, $^{***}P < 0.001$. Symbols and bars indicated the means ± SD.

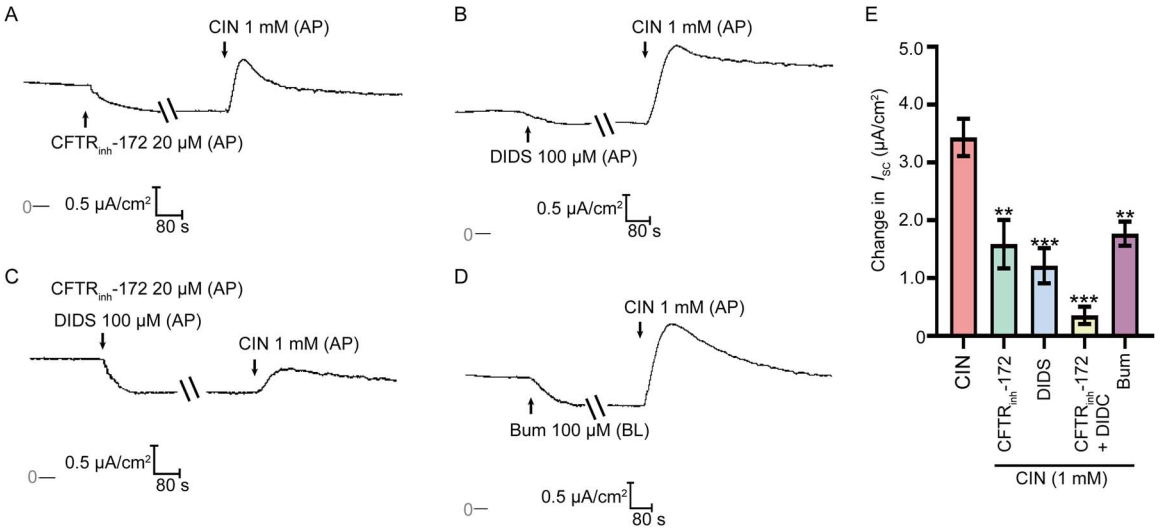

Figure 4. Involvement of CFTR and CaCC in the TRPA1 activation-stimulated anion secretion. (A)–(D) Representative trace showing the effect of CFTRinh-172 (20 μM, AP), or/and DIDS (100 μM, AP), or NKCC inhibitor bumetanide (100 μM, BL) pretreatment on the I_{SC} responses induced by CIN (1 mM, AP). (E) Statistical analysis showing the I_{SC} responses elicited by CIN in different conditions ($n = 4$–6). $^{**}P < 0.01$, $^{***}P < 0.001$ versus the CIN group. Symbols and bars indicated the means ± SD.

to better reproductive health in obese male individuals [31]. However, the underlying mechanism of HFD and physical exercises on the secretion functions of epididymal epithelium remains unknown. Herein, we uncovered the benefit effect of physical exercises on the secretion function of epididymal epithelium in HFD-induced obese rats for the first time. Notably, 12 weeks of regular aerobic exercises reversed the downregulated the TRPA1 expression level in the epididymal epithelium of HFD-induced obese rats and improved the dysfunction of anion homeostasis in the epididymal fluid

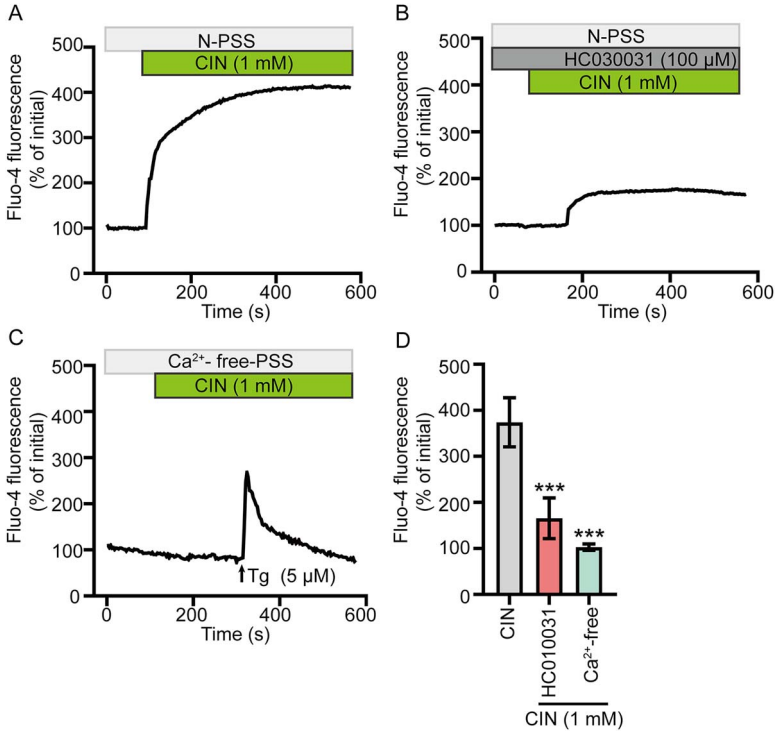

Figure 5. Activation of TRPA1 induced the Ca^{2+} influx of rat epididymal epithelial cells. (A)–(C) Fluo-4 fluorescence was measured to detect the Ca^{2+} responses elicited by CIN (1 mM) in (A) NPSS, (B) in the presence of HC030031 (100 μM) or in (C) Ca^{2+}-free PSS. Tg (5 μM) were used as positive controls. (D) Statistical analysis showing the CIN-stimulated Ca^{2+} responses in various conditions ($n = 5$). $^{***}P < 0.001$ versus the CIN group. Symbols and bars indicated the means ± SD.

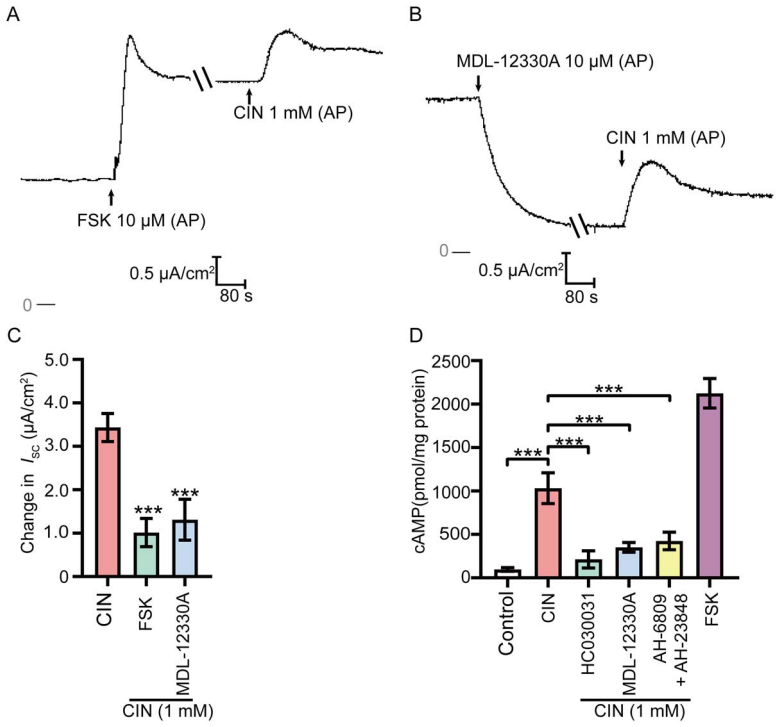

Figure 6. Involvement of adenosine cyclase (AC)-cAMP pathway in the TRPA1 activation-stimulated anion secretion. (A) and (B) Representative recordings of the *I*sc responses induced by CIN (1 mM, AP) with the pretreatment of AC agonist FSK (10 μM, AP) or AC inhibitor MDL-12330A (10 μM, AP). (C) Statistical analysis showing the I_{SC} responses elicited by CIN in different conditions ($n = 4$–6), $^{***}P < 0.001$ versus the CIN group. (D) Statistical analysis showing the CIN (1 mM) stimulated cAMP synthesis of epididymis epithelial cells in different conditions ($n = 4$). $^{***}P < 0.001$. Symbols and bars indicated the means ± SD.

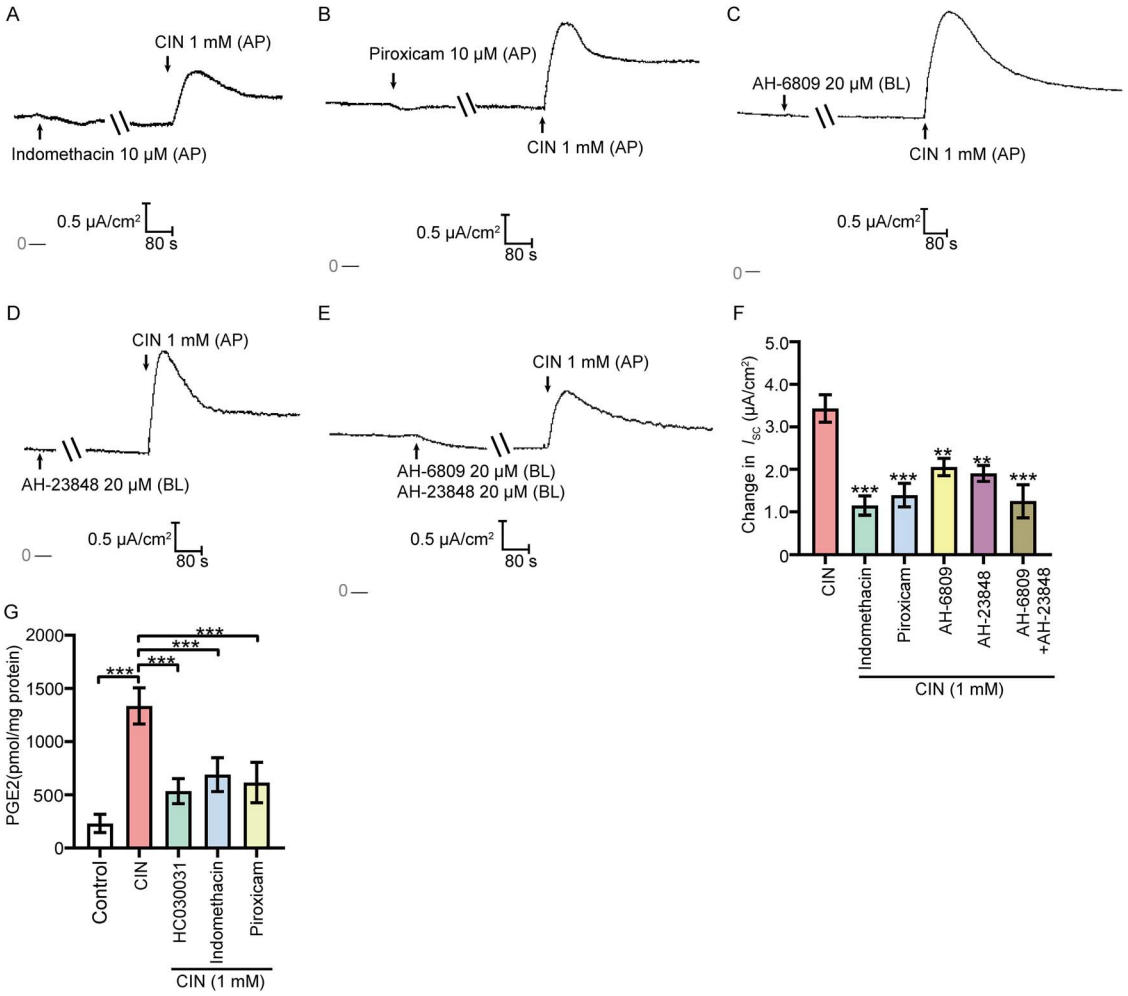

Figure 7. Involvement of PGHS2-PGE2-EP2/EP4 pathway in the TRPA1 activation-stimulated anion secretion. (A) and (B) Representative recordings of the *I*sc responses induced by CIN (1 mM, AP) when pretreating the epithelial cells with PGHS2 inhibitors indomethacin (10 μM, AP) or piroxicam (10 μM, AP). (C)–(E) Representative recordings of CIN -stimulated *I*sc responses when pretreating the epithelial cells with AH-6809 (20 μM, BL) or /and AH-23848 (20 μM, BL). (F) Statistical analysis showing the I_{SC} responses elicited by CIN in different conditions ($n = 4$–6), $^{**}P < 0.01$, $^{***}P < 0.001$ versus the CIN group. (G) Statistical analysis showing the CIN (1 mM) stimulated PGE2 synthesis of epididymis epithelial cells in different conditions ($n = 4$). $^{***}P < 0.001$. Symbols and bars indicated the means ± SD.

and the decline of sperm fertilizing ability. Moreover, we uncovered that activation of TRPA1 promoted the transepithelial secretion of Cl^- and HCO_3^- via the Ca^{2+}-CaCC and Ca^{2+}-PGHS2-PGE2-cAMP-CFTR pathways. The proposed working model is illustrated in Figure 8.

TRPA1 was originally detected in the sensory neurons [32]. Its expression in non-neuronal cells was observed recently [27, 33]. Though positive immunoreactivity has been observed in the epithelial and subepithelial cells in the rat colon [26], the expression pattern of TRPA1 in the male reproductive system remains unknown. In this study, the immunolabeling of TRPA1 in rat epididymis was detected in epididymal epithelial layer (Figure 2A–D). TRPA1 is originally known for its role in pain sensation. Recently, growing evidence suggested TRPA1 was also involved in metabolic and pro-secretion functions. Besides, numerous studies have reported that TRPA1 plays important roles in the pathological processes of diet-induced obese individuals and possesses potential therapeutic value [20, 34, 35]. For instance, diet-induced obesity has been reported to reduce the TRPA1 protein expression level in the trigeminal ganglia and gut [24, 25]. In contrast, an increased expression of TRPA has been reported in obese Zucker rats, inducing bladder dysfunction [23]. In this study, the expression level of TRPA1 in the epididymal epithelium was downregulated in the HFD-induced obese rats (Figure 1E–G). These findings suggested disparities in the effect of diet-induced obesity on the TRPA1 protein expression in different species and tissues. Nonetheless, we found that regular physical exercises can improve the disorders of TRPA1 protein expression pattern of HFD-induced obese rats. Besides, our data showed that significant increasement of TRPA1 expression level was not detected in the NE group, suggesting that TRPA1 maybe not the direct target of aerobic exercises. Hence, the underlying mechanism of aerobic exercise reverse the decline of TRPA1 expression level induced by HFD needs further investigation.

Over the past decades, obesity has become a major health problem facing human beings, and the health risks of obesity and overweight show a tendency to rise worldwide [36]. Dysfunction of the male reproductive system is one of the complications of obesity. Although not all obese male individuals necessarily have impaired reproductive ability, the clinical data showed that nearly 80% of male patients with reproductive disorders are classified as overweight or obesity [10].

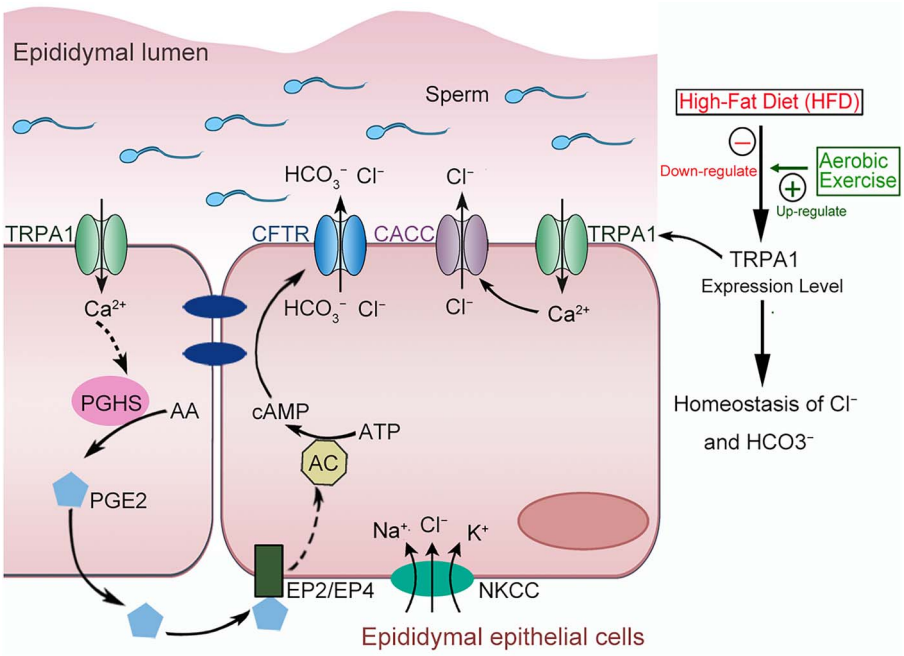

Figure 8. *Proposed working model of aerobic exercises regulates the anion homeostasis in epididymal lumen of HFD-induced obese rat through TRPA1-mediated Cl^- and $HCO3^-$ secretion.* Aerobic exercises could reverse the downregulation of TRPA in epididymal epithelium of obesity rats and recover the anion homeostasis in the fluid milieu of rat cauda epididymis. Activation of TRPA1 stimulates a Ca^{2+} influx and then induce a transepithelial Cl^- and HCO_3^- secretion through activating CFTR and CACC channels.

Obesity adversely affects male reproduction, including spermatogenesis in the testis and the subsequent sperm maturation process in the epididymis, leading to decreased sperm concentration, abnormal morphology of the sperm, impaired sperm motility and fertilizing capacity [3, 37, 38]. Previous studies reported that obesity affected the activity of the hypothalamic–pituitary–testis axis, thus damaging spermatogenesis [39, 40]. Notably, obese individuals usually have lower sperm motility and fertilizing capacity, suggesting that obesity affects the sperm maturation process in the epididymis. However, the adverse effects of obesity on the epididymis have often been overlooked. In mammals, sperm sequentially acquire their fertilizing capacity and forward motility relying on the appropriate epididymal intraluminal microenvironment. Herein, we found that the Cl^- concentration in the epididymal lumen fluid were significantly decreased, the sperm motility and capacitation ability were also significantly impaired in HED-induced obese rats (Figure 1A–D, & F), suggesting the disorder of the epididymal luminal milieu. Similarly, the expression level of TRPA1 was decreased in the epididymal epithelium of HED-induced obese rats. These findings suggested a possible connection between TRPA1 expression level and the Cl^- concentration in the epididymal lumen fluid.

The pro-secretion function of TRPA1 in the colon has been demonstrated in various species [26, 27, 41]. However, the functional expression of TRPA1 in the epididymis remains elusive. In this study, our I_{SC} experiments revealed that TRPA1 activation stimulated a significant secretion of Cl^- and HCO_3^- (Figures 2 and 3). In line with the pro-secretion function of TRPA1 in the colon, the activation of CFTR was a downstream event of TRPA1 activation (Figure 4). CFTR is a cAMP-regulated channel that ensures transepithelial transport of Cl^- and HCO_3^- [30, 42]. AC activation is an important upstream cellular event before the opening of CFTR. TRPA1 activation by luminal stimuli induces EP4-AC-cAMP-mediated CFTR activation in human and rat colons. In this study, TRPA1 activation triggered the elevation of [cAMP]i through the EP2/EP4-AC pathway (Figure 6). EP2 and EP4 are the receptors of the endogenous epithelium-derived factor PGE2. The findings herein demonstrated that TRPA1 activation stimulated increased PGE2 synthesis by the activation of PGHS2 in epididymal epithelial cells (Figure 7 G). As is known, PGHS2 is activated by the elevation of $[Ca^{2+}]_i$ [43]. Our data showed that activation of the calcium-permeable TRPA1 channel stimulated a Ca^{2+} influx and the subsequent elevation of $[Ca^{2+}]_i$ (Figure 5), suggesting that TRPA1 activation caused a significant increase in the PGHS2-dependent synthesis of PGE2. PGE2 subsequently acted on EP2 and EP4 receptors of the epithelial cells, leading to the accumulation of intracellular cAMP by activating AC, which in turn triggered Cl^- and HCO_3^- secretion via CFTR. Moreover, an increase in $[Ca^{2+}]$i could trigger the activation of CaCC (Figure 5), which was different from the pro-secretion function of TRPA1 in the colon. These studies highlight the pleiotropic functions of TRPA1 in different epithelial tissues.

Ion homeostasis of the epididymal lumen is vital for sperm maturation. Our previous study demonstrated that dysfunction of K^+ homeostasis in the fluid milieu of rat cauda epididymis leads to a decline in sperm motility [18]. The dysbiosis of Cl^-, HCO_3^-, and Ca^{2+} in the epididymal fluid has also been reported to impair sperm motility. Sperm motility is regulated by HCO_3^-, Ca^{2+}, and Cl^- influxes, which trigger biochemical and electrophysiological changes in the cytoplasm and the entire plasma membrane of the sperm cells [44]. TRPV6 gene deficiency results in the dysfunction of Ca^{2+} absorption, leading to the Ca^{2+} concentration in cauda epididymis being ten times higher than that of wild-type mice.

This phenomenon is associated with reduced sperm viability in cauda epididymis [19, 45]. Obstructing of the Cl^- and HCO_3^- secretion induced by Slc26a3 deficiency is associated with impaired sperm fertilization in the mice epididymis [46]. A close relationship between Cl^-, HCO_3^-, and sperm capacitation ability in rat has also been reported [47]. In this study, we found that HFD induced dysbiosis of Cl^- and HCO_3^- in the fluid milieu, and thus impaired the fertilizing capacity of rat cauda epididymis. However, these phenomena were reversed after 12 weeks of regular aerobic exercises. These data suggested that TRPA1 play important role in the anion homeostasis regulation in rat epididymis. Nonetheless, tissue-specific knockout of TRPA1 in rat epididymis should be used to further evaluate its functional role in male fertility.

Conclusion

This study highlights the role of physical exercises in reversing the downregulated TRPA1 expression level in the epididymal epithelium of HFD-induced obese rats, and reveal its subsequent involvement in the transepithelial secretion and homeostasis regulation of Cl^- and HCO_3^- in the fluid milieu of rat cauda epididymis. TRPA1 in the epididymal epithelium is thus a potential target of diet-induced obesity and physical exercises, providing new insight for diagnosing and treating asthenospermia caused by obesity.

Conflict of Interest

There is no conflict of interest that could be perceived as prejudicing the impartiality of the research reported.

Data availability

The data used to support the findings of this study are available from the corresponding author upon request.

Author contributions

Dong-Dong Gao, Jun-Hao Huang, and Min Hu: conception and design of the work; Dong-Dong Gao, Nan Ding, Wei-Ji Deng, Pei-Lun Li, Yi-Lin Chen, Lian-Meng Guo, Wen-Hao Liang, Jia-Hui Zhong, and Jing-Wen Liao: establishment of the rat models, acquisition, analysis, or interpretation of data; Dong-Dong Gao: article writing with contributions from other authors. Jun-Hao Huang and Min Hu revised the manuscript. All authors approved the final manuscript and agreed to be accountable for the work. All persons designated as authors qualify for authorship, and all those who qualify for authorship are listed.

References

1. Hammoud AO, Wilde N, Gibson M, Parks A, Carrell DT, Meikle AW. Male obesity and alteration in sperm parameters. *Fertil Steril* 2008; **90**:2222–2225.
2. Bakos HW, Henshaw RC, Mitchell M, Lane M. Paternal body mass index is associated with decreased blastocyst development and reduced live birth rates following assisted reproductive technology. *Fertil Steril* 2011; **95**:1700–1704.
3. Leisegang K, Sengupta P, Agarwal A, Henkel R. Obesity and male infertility: mechanisms and management. *Andrologia* 2021; **53**:e13617.
4. Craig JR, Jenkins TG, Carrell DT, Hotaling JM. Obesity, male infertility, and the sperm epigenome. *Fertil Steril* 2017; **107**:848–859.
5. Heydari H, Ghiasi R, Ghaderpour S, Keyhanmanesh R. The mechanisms involved in obesity-induced male infertility. *Curr Diabetes Rev* 2021; **17**:259–267.
6. Khodamoradi K, Parmar M, Khosravizadeh Z, Kuchakulla M, Manoharan M, Arora H. The role of leptin and obesity on male infertility. *Curr Opin Urol* 2020; **30**:334–339.
7. Agarwal A, Rana M, Qiu E, AlBunni H, Bui AD, Henkel R. Role of oxidative stress, infection and inflammation in male infertility. *Andrologia* 2018; **50**:e13126.
8. Ding N, Zhang X, Zhang XD, Jing J, Liu SS, Mu YP, Peng LL, Yan YJ, Xiao GM, Bi XY, Chen H, Li FH, *et al.* Impairment of spermatogenesis and sperm motility by the high-fat diet-induced dysbiosis of gut microbes. *Gut* 2020; **69**:1608–1619.
9. Celik O, Yildiz BO. Obesity and physical exercise. *Minerva Endocrinol (Torino)* 2021; **46**:131–144.
10. Palmer NO, Bakos HW, Owens JA, Setchell BP, Lane M. Diet and exercise in an obese mouse fed a high-fat diet improve metabolic health and reverse perturbed sperm function. *Am J Physiol Endocrinol Metab* 2012; **302**:E768–E780.
11. Rafiee B, Morowvat MH, Rahimi-Ghalati N. Comparing the effectiveness of dietary vitamin C and exercise interventions on fertility parameters in normal obese men. *Urol J* 2016; **13**:2635–2639.
12. Nematollahi A, Kazeminasab F, Tavalaee M, Marandi SM, Ghaedi K, Nazem MN, Nasr-Esfahani MH. Effect of aerobic exercise, low-fat and high-fat diet on the testis tissue and sperm parameters in obese and nonobese mice model. *Andrologia* 2019; **51**:e13273.
13. Heydari H, Ghiasi R, Hamidian G, Ghaderpour S, Keyhanmanesh R. Voluntary exercise improves sperm parameters in high fat diet receiving rats through alteration in testicular oxidative stress, mir-34a/SIRT1/p53 and apoptosis. *Horm Mol Biol Clin Investig* 2021; **42**:253–263.
14. Mu Y, Dai HG, Luo LB, Yang J. Irisin alleviates obesity-related spermatogenesis dysfunction via the regulation of the AMPKα signalling pathway. *Reprod Biol Endocrinol* 2021; **19**:135.
15. Martini AC, Tissera A, Estofán D, Molina RI, Mangeaud A, de Cuneo MF, Ruiz RD. Overweight and seminal quality: a study of 794 patients. *Fertil Steril* 2010; **94**:1739–1743.
16. Fernandes GS, Arena AC, Campos KE, Volpato GT, Anselmo-Franci JA, Damasceno DC, Kempinas WG. Glutamate-induced obesity leads to decreased sperm reserves and acceleration of transit time in the epididymis of adult male rats. *Reprod Biol Endocrinol* 2012; **10**:105.
17. Hinton BT, Palladino MA. Epididymal epithelium: its contribution to the formation of a luminal fluid microenvironment. *Microsc Res Tech* 1995; **30**:67–81.
18. Gao DD, Xu JW, Qin WB, Peng L, Qiu ZE, Wang LL, Lan CF, Cao XN, Xu JB, Zhu YX, Tang YG, Zhang YL, *et al.* Cellular mechanism underlying hydrogen Sulfide mediated epithelial K(+) secretion in rat epididymis. *Front Physiol* 2018; **9**:1886.
19. Weissgerber P, Kriebs U, Tsvilovskyy V, Olausson J, Kretz O, Stoerger C, Vennekens R, Wissenbach U, Middendorff R, Flockerzi V, Freichel M. Male fertility depends on Ca^2+ absorption by TRPV6 in epididymal epithelia. *Sci Signal* 2011; **4**:ra27.
20. Derbenev AV, Zsombok A. Potential therapeutic value of TRPV1 and TRPA1 in diabetes mellitus and obesity. *Semin Immunopathol* 2016; **38**:397–406.
21. Zhu H, Wang Y, He Y, Yu W. Inflammation-mediated macrophage polarization induces TRPV1/TRPA1 heteromers in endometriosis. *Am J Transl Res* 2022; **14**:3066–3078.
22. Saha S, Sucharita S, Majhi RK, Tiwari A, Ghosh A, Pradhan SK, Patra BK, Dash RR, Nayak RN, Giri SC, Routray P, Kumar A, *et al.* TRPA1 is selected as a semi-conserved channel during vertebrate evolution due to its involvement in spermatogenesis. *Biochem Biophys Res Commun* 2019; **512**:295–302.
23. Blaha I, López-Oliva ME, Martínez MP, Recio P, Agis-Torres Á, Martínez AC, Benedito S, García-Sacristán A, Prieto D, Fernandes

VS, Hernández M. Bladder dysfunction in an obese Zucker rat: the role of TRPA1 channels, oxidative stress, and hydrogen sulfide. *Oxid Med Cell Longev* 2019; **2019**:5641645.
24. Marics B, Peitl B, Varga A, Pázmándi K, Bácsi A, Németh J, Szilvássy Z, Jancsó G, Dux M. Diet-induced obesity alters dural CGRP release and potentiates TRPA1-mediated trigeminovascular responses. *Cephalalgia* 2017; **37**:581–591.
25. Khare P, Mahajan N, Singh DP, Kumar V, Kumar V, Mangal P, Boparai RK, Gesing A, Bhadada SK, Sharma SS, Kondepudi K, Chopra K, *et al*. Allicin, a dietary trpa1 agonist, prevents high fat diet-induced dysregulation of gut hormones and associated complications. *Food Funct* 2021; **12**:11526–11536.
26. Kaji I, Yasuoka Y, Karaki S, Kuwahara A. Activation of TRPA1 by luminal stimuli induces EP4-mediated anion secretion in human and rat colon. *Am J Physiol Gastrointest Liver Physiol* 2012; **302**:G690–G701.
27. Manneck D, Manz G, Braun HS, Rosendahl J, Stumpff F. The TRPA1 agonist Cinnamaldehyde induces the secretion of HCO(3)(−) by the porcine colon. *Int J Mol Sci* 2021; **22**:5198.
28. Gao DD, Lan CF, Cao XN, Chen L, Lei TL, Peng L, Xu JW, Qiu ZE, Wang LL, Sun Q, Huang ZY, Zhu YX, *et al*. G protein-coupled estrogen receptor promotes acrosome reaction via regulation of Ca2+ signaling in mouse spermdagger. *Biol Reprod* 2022; **107**: 1026–1034.
29. Gao DD, Wang LL, Xu JW, Qiu ZE, Zhu YX, Zhang YL, Zhou WL. Cellular mechanism underlying oxytocin-stimulated Cl(−) secretion in rat cauda epididymal epithelium. *Am J Physiol Cell Physiol* 2020; **319**:C630–C640.
30. Peng L, Gao DD, Xu JW, Xu JB, Ke LJ, Qiu ZE, Zhu YX, Zhang YL, Zhou WL. Cellular mechanisms underlying carbon monoxide stimulated anion secretion in rat epididymal epithelium. *Nitric Oxide* 2020; **100-101**:30–37.
31. Sansone A, Sansone M, Vaamonde D, Sgrò P, Salzano C, Romanelli F, Lenzi A, Di Luigi L. Sport, doping and male fertility. *Reprod Biol Endocrinol* 2018; **16**:114.
32. Bautista DM, Movahed P, Hinman A, Axelsson HE, Sterner O, Hogestatt ED, Julius D, Jordt SE, Zygmunt PM. Pungent products from garlic activate the sensory ion channel TRPA1. *Proc Natl Acad Sci USA* 2005; **102**:12248–12252.
33. De Logu F, Li Puma S, Landini L, Portelli F, Innocenti A, de Araujo DSM, Janal MN, Patacchini R, Bunnett NW, Geppetti P, Nassini R. Schwann cells expressing nociceptive channel TRPA1 orchestrate ethanol-evoked neuropathic pain in mice. *J Clin Invest* 2019; **129**: 5424–5441.
34. Zuo J, Zhao D, Yu N, Fang X, Mu Q, Ma Y, Mo F, Wu R, Ma R, Wang L, Zhu R, Liu H, *et al*. Cinnamaldehyde ameliorates diet-induced obesity in mice by inducing Browning of white adipose tissue. *Cell Physiol Biochem* 2017; **42**:1514–1525.
35. Tamura Y, Iwasaki Y, Narukawa M, Watanabe T. Ingestion of cinnamaldehyde, a TRPA1 agonist, reduces visceral fats in mice fed a high-fat and high-sucrose diet. *J Nutr Sci Vitaminol (Tokyo)* 2012; **58**:9–13.
36. Caballero B. Humans against obesity: who will win? *Adv Nutr* 2019; **10**:S4–s9.
37. Kahn BE, Brannigan RE. Obesity and male infertility. *Curr Opin Urol* 2017; **27**:441–445.
38. Bunay J, Gallardo LM, Torres-Fuentes JL, Aguirre-Arias MV, Orellana R, Sepúlveda N, Moreno RD. A decrease of docosahexaenoic acid in testes of mice fed a high-fat diet is associated with impaired sperm acrosome reaction and fertility. *Asian J Androl* 2021; **23**: 306–313.
39. Chang B, Song C, Gao H, Ma T, Li T, Ma Q, Yao T, Wang M, Li J, Yi X, Tang D, Cao S. Leptin and inflammatory factors play a synergistic role in the regulation of reproduction in male mice through hypothalamic kisspeptin-mediated energy balance. *Reprod Biol Endocrinol* 2021; **19**:12.
40. Liu RR, Zhang HQ. Expression of the kisspeptin/kiss1r system in the hypothalamic arcuate nucleus of rats with diet-induced obesity and its influence on the hypothalamic-pituitary-testis axis. *Zhonghua Nan Ke Xue* 2014; **20**:792–797.
41. Tsuchiya Y, Kawamata K. Allicin induces electrogenic secretion of chloride and bicarbonate ions in rat colon via the TRPA1 receptor. *J Nutr Sci Vitaminol (Tokyo)* 2019; **65**:258–263.
42. Cao X, Huang J, Zhang G, Zuo W, Lan C, Sun Q, Yang D, Gao D, Cheng CH, Zhou WL. Functional expression of G protein-coupled receptor 30 in immature rat epididymal epithelium. *Cell Biol Int* 2017; **41**:134–146.
43. Ruan YC, Wang Z, Du JY, Zuo WL, Guo JH, Zhang J, Wu ZL, Wong HY, Chung YW, Chan HC, Zhou WL. Regulation of smooth muscle contractility by the epithelium in rat vas deferens: role of ATP-induced release of PGE2. *J Physiol* 2008; **586**:4843–4857.
44. Touré A. Importance of SLC26 transmembrane anion exchangers in sperm post-testicular maturation and fertilization potential. *Front Cell Dev Biol* 2019; **7**:230.
45. Gao da Y, Zhang BL, Leung MC, Au SC, Wong PY, Shum WW. Coupling of TRPV6 and TMEM16A in epithelial principal cells of the rat epididymis. *J Gen Physiol* 2016; **148**:161–182.
46. El Khouri E, Whitfield M, Stouvenel L, Kini A, Riederer B, Lores P, Roemermann D, di Stefano G, Drevet JR, Saez F, Seidler U, Touré A. Slc26a3 deficiency is associated with epididymis dysplasia and impaired sperm fertilization potential in the mouse. *Mol Reprod Dev* 2018; **85**:682–695.
47. Jin JY, Chen WY, Zhou CX, Chen ZH, Yu-Ying Y, Ni Y, Chan HC, Shi QX. Activation of GABAA receptor/Cl- channel and capacitation in rat spermatozoa: HCO_3^- and Cl- are essential. *Syst Biol Reprod Med* 2009; **55**:97–108.